JOURNAL OF CATALYSIS **110**, 23–36 (1988)

Surface Structure and Catalytic Properties of the MoO_3–MgF_2 System

JERZY HABER* AND MARIA WOJCIECHOWSKA†

**Institute of Catalysis and Surface Chemistry, Polish Academy of Sciences, Kraków, and †Institute of Chemistry, A. Mickiewicz University, Poznań, Poland*

Received December 3, 1986; revised June 16, 1987

IR, ESR, and XRD studies of MoO_3–MgF_2 samples revealed the existence of two types of complexes on the surface of the MgF_2 support, namely, isolated MoO_3 tetrahedra and clusters of MoO_6 octahedra of the MoO_3 structure. Changes in the degree of hydroxylation of the magnesium fluoride surface after impregnation with molybdate ions were followed by IR spectroscopy. Determination of acid–base properties by means of probe molecules such as pyridine and acetic acid enabled the origin of the acid centres to be explained. The appearance of new acid–base and redox centers in MoO_3–MgF_2 samples is responsible for their activity in many catalytic reactions.

INTRODUCTION

As a result of the interaction of MgF_2 with oxidizing acids of chlorine, sulfur, phosphorus, and boron (*1–3*), a considerable increase of the surface area takes place and Lewis-type acid centers of considerable strength are formed. These centers are responsible for catalytic activity in model reactions taking place on acid centers of various strengths. Attempts to introduce silicic acid on freshly precipitated magnesium fluoride did not bring about the expected changes in acidity of MgF_2 (*3*); however, introduction of ammonium molybdate generated remarkable changes in the surface properties of MgF_2.

The high activity of MoO_3–MgF_2 preparations, compared with the limited activity of magnesium fluoride (*4*), indicated the appearance of new active centers in the presence of MoO_3 which may be related to the formation of surface hydroxyl groups. During the dehydroxylation of such samples, acid and base centers of Lewis type may be formed.

It therefore seemed interesting to undertake a study of the structure of the MgF_2 surface on which Mo–O polyhedra were deposited and to elucidate the mechanism of generation of the active centers responsible for their catalytic properties.

EXPERIMENTAL

Magnesium fluoride was obtained by adding small portions of $MgCO_3 \cdot 3H_2O$ to a 20% aqueous solution of hydrofluoric acid until neutralization, and acidifying by introducing a few additional drops of the acid. A hot aqueous solution of $(NH_4)_2MoO_4$ was then introduced to the precipitate of MgF_2 in quantities corresponding to the following Mo/Mg atomic ratios: 0.01, 0.05, 0.10, 0.18, and 0.25.[1] When thoroughly mixed, the precipitate was left for 24 h; dried for 25 h, first at 50–70°C and then at 105°C; and finally calcined at 400°C for 5 h. The MoO_3 sample was obtained by thermal decomposition of ammonium molybdate (5h at 400°C).

The surface area was determined by a gravimetric method using a Sartorius Gravimat with nitrogen as the adsorbate at −195°C. IR spectra were recorded with a Perkin-Elmer Model 580 double-beam spectrophotometer in the range of free lattice vibrations and the stretching range of OH

---

[1] These samples hereafter will be denoted by the symbols $MFMo_X$, where X is 100 × Mo/Mg atomic ratio; e.g., a MoO_3–MgF_2 sample with Mo/Mg atomic ratio 0.05 is designated $MFMo_5$.

0021-9517/88 $3.00

groups, as well as the region of the stretching and deformation vibrations of adsorbed molecules. For examination within the range 350–1300 cm^{-1}, samples were prepared by pelleting the catalyst with CsBr. IR examinations within the range 4000–1400 cm^{-1} were carried out using a vacuum cell equipped with sodium chloride windows. The samples in the form of thin disks were evacuated at 10^{-3} Pa for 5 h at 400°C and cooled to room temperature, and the spectrum was recorded. Then, pyridine vapor was admitted to the cell at 200°C and after 0.5 h the cell was evacuated for 2 h at this temperature.

IR examination of the adsorption of acetic acid was carried out in a similar way. The acid was adsorbed at 150 and 250°C, and then desorbed at these temperatures.

ESR measurements were made with a SE/X-2542 Radiopan-Spectrometer (X-band, $\nu \approx 9.4$ GHz) at room temperature and in liquid nitrogen (77 K). DPPH was used as the external reference standard for the g value ($g_{\mathrm{DPPH}} = 2.0036$). Samples for ESR examination were prepared in two ways: (1) an additionally calcined sample (2 h at 350°C) was placed into a quartz tube and sealed instantly (oxidized sample); (2) a sample was first annealed in oxygen and then degassed at 400°C for 3 h (reduced sample).

Catalytic properties were determined by the pulse microreactor technique in the following reactions: skeletal isomerization of cyclohexene at 370°C, cumene cracking at 320°C, and butene isomerization at 200°C. Conditions for the catalytic measurements were similar to those described elsewhere (*5*, *6*), except that 0.1 g of a catalyst was used for each of these reactions. Catalytic activity was expressed in terms of the kK product of the Bassett–Habgood equation (*7*).

The activity of the samples in toluene ammoxidation was determined by the pulse microreactor technique as follows: Measurements were carried out at 400°C with a ratio of toluene : oxygen : NH_3 of 1 : 3 : 1. Helium was used as carrier gas; its flow rate was 42 ml/min, and the toluene flow rate was 1.9 ml/min. Liquid reaction products were analyzed chromatographically by use of a 1-m column packed with Carbowax 1000, at two temperatures, viz., 65 and 122°C. At the lower temperature air, ammonia, benzene, toluene, and water were separated. By applying temperature programming up to 122°C the benzonitrile peak was obtained. Separation of gas products was carried out on a 2-m column packed with active carbon.

The coke formed on the catalyst was determined from the weight difference after combustion of the sample of 600°C in oxygen for 1 h (the water content in the sample was taken into consideration).

X-ray examination was carried out with a M-62 diffractometer in conjunction with a HZG-3 powder goniometer, and Ni-filtered CuK_{α} radiation was used.

RESULTS AND DISCUSSION

Table 1 presents Mo/Mg atomic ratios and surface areas of the investigated sam-

TABLE 1

Sample Characterization

Sample	MF	$MFMo_1$	$MFMo_5$	$MFMo_{10}$	$MFMo_{18}$	$MFMo_{25}$	MoO_3
Atom ratio Mo/Mg	0.00	0.01	0.05	0.10	0.18	0.25	
Surface area (m^2/g)	46.0	50	69	123	96	66	3.4
Protonic acidity/aprotonic acidity ratio (350°C)	0.0	0.0	0.2	0.7	0.8	0.2	

ples as well as the protonic : aprotonic acidity ratio determined on the basis of the intensity of appropriate bands in the IR spectra.

The results of the surface area measurements indicate that introduction of ammonium molybdate causes an increase in the surface area. Maximum surface area was obtained for the $MFMo_{10}$ preparation. It was 123 m^2/g, i.e., almost three times that of the MgF_2 sample not impregnated with ammonium molybdate. Ammonia and water evolved during thermal treatment of the catalyst induce "fluffing" of the preparation, thus favorably affecting the pore system. The surface areas of $MFMo_{18}$ and $MFMo_{25}$ were lower than that of $MFMo_{10}$, probably because of the larger contribution to the total surface area from MoO_3 itself. A microporous system is not well developed in MoO_3; thus, its surface area is only 3.4 m^2/g.

Figure 1 presents IR spectra of MoO_3–MgF_2 preparations and of pure MgF_2 and MoO_3. MoO_3–MgF_2 preparations are characterized not only by bands specific to pure MgF_2 but also by a broad, intense band with a maximum at 880–895 cm^{-1} and a band at 930 cm^{-1}. For $MFMo_{10}$, $MFMo_{18}$, and $MFMo_{25}$ an additional band appears at 985 cm^{-1}, and for $MFMo_{18}$ and $MFMo_{25}$ there is a further band at 870 cm^{-1}. On the basis of the known characteristic vibrations of the $[MoO_4]$ group in which Mo is tetrahedrally coordinated (*8–10*), as well as from comparison with the spectra of MgF_2 and MoO_3 (spectra 1 and 7, respectively in Fig. 1), it may be concluded that the bands at 930 and 880–895 cm^{-1} originate from the tetrahedral ion $[MoO_4]$. This assignment is confirmed by the results of IR examination of $MgMoO_4$ (calcined at 400 and 600°C) and $Na_2MoO_4 \cdot 2H_2O$ (*9*), in which molybdate ions are in a tetrahedral coordination. Both preparations showed bands at 930 and 895 cm^{-1}. Hence, the appearance of these bands may be taken as an indication of the presence of molybdate ions in tetrahedral coordination in the examined preparations. Besides the bands characteristic of the $[MoO_4]$ ion, bands characteristic of MoO_3 were also observed (985 and 870 cm^{-1}, corresponding to vibrations of Mo=O and Mo—O—Mo, respectively). Their presence was also detected in $MFMo_1$ and $MFMo_5$ but only after doubling the weight of the sample. The intensity of the bands characteristic of the $[MoO_4]$ groups and MoO_3 increases as the Mo/Mg ratio in the samples increases.

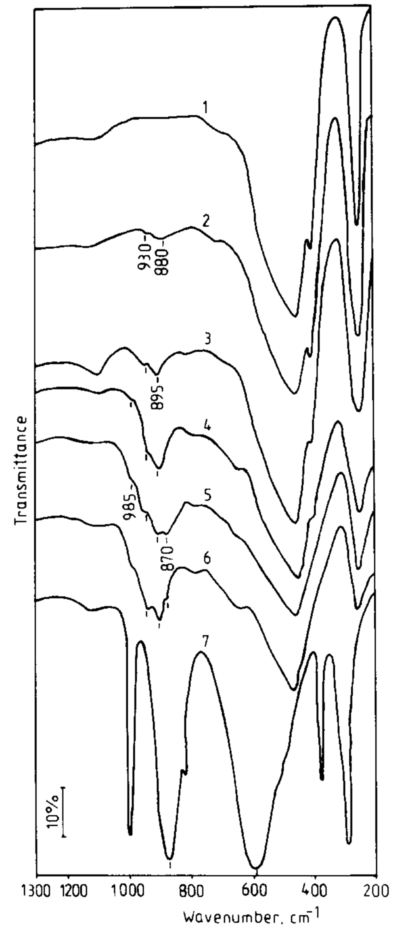

FIG. 1. IR spectra of magnesium fluoride impregnated with ammonium molybdate. (1) MgF_2, (2) $MFMo_1$, (3) $MFMo_5$, (4) $MFMo_{10}$, (5) $MFMo_{18}$, (6) $MFMo_{25}$, (7) MoO_3.

X-ray examination indicated that in MoO_3–MgF_2 preparations only MoO_3 and MgF_2 are present; no line characteristic of molybdate could be detected. The lack of the latter may be due either to the new phase produced as a result of the interaction of molybdate ions with the surface of MgF_2 being amorphous or to the low sensitivity of the X-ray analysis.

The absence of the $MgMoO_4$ phase was confirmed by the results of an experiment in which a mixture of MoO_3 and MgF_2 (1 : 1 molar ratio) was calcined a 400 and 600°C for 5 h. XRD revealed $MgMoO_4$ only in the sample calcined at 600°C, whereas in the IR spectra of both samples two bands at 930 and 895 cm^{-1} characteristic of the $[MoO_4]$ ions appeared. The fact that these bands are less intense in the sample resulting from the solid-state reaction of the MgF_2 and MoO_3 mixture at 400°C than in the MoO_3–MgF_2 preparations obtained by impregnation may be explained by the much higher surface area of the latter.

More detailed information on the surface structure of MoO_3-promoted preparations was provided by ESR studies. They were carried out for samples $MFMo_1$ and $MFMo_5$. Spectra of oxidized samples recorded at room and liquid nitrogen temperatures did not reveal the presence of Mo(V) ions. The reduced samples produced ESR spectra indicating the appearance of Mo(V) ions. The most distinct spectrum was obtained for $MFMo_5$ at liquid nitrogen temperature (Fig. 2). It is an intense axial spectrum with easily discernible $g_\perp$ and $g_\parallel$ parameters and with well-pronounced components of hyperfine structure in the perpendicular orientation. The spectrum of $MFMo_1$ was slightly weaker and its degree of asymmetry lower. Parameters of this spectrum, namely $g_\perp = 1.940$, $g_\parallel = 1.875$ (± 0.002), and $A_\perp \approx 50$ Gs, are identical to those assigned to Mo(V) complexes of square pyramidal C_{4v} symmetry with oxygen ligands ($g_\perp > g_\parallel$) in the reduced catalyst MoO_3/SiO_2 (*11*). A similar spectrum was described in other papers (*12, 13*) in which it was attributed to type A Mo(V) centers formed in the initial stage of MoO_3 reduction. It is composed of Mo ions with the symmetry of a distorted rhombic pyramid.

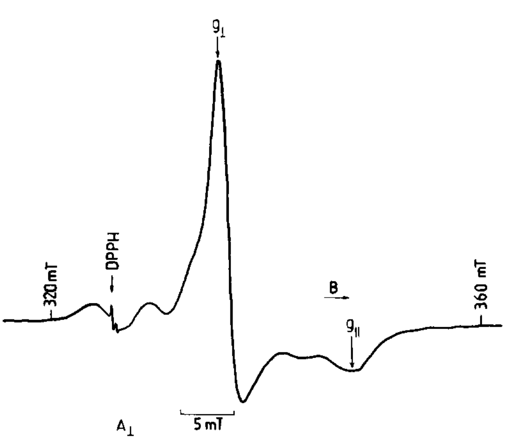

FIG. 2. ESR spectra of reduced $MFMo_5$ sample (at liquid nitrogen temperature).

Comparison of IR and ESR results obtained for MgF_2 samples modified with ammonium molybdate enables some conclusions to be drawn concerning the structure of the surface species. As seen from the IR spectra (Fig. 1), the preparations studied show the existence of bands characteristic of MoO_3 as well as bands indicating the occurrence of $[MoO_4]$ species with tetrahedrally coordinated Mo. They form nearly regular tetrahedra with small differences in O–Mo–O angles and in Mo–O distances. In such a regular coordination the Mo(V) cannot be observed by ESR. If the $[MoO_4]$ complexes interacted with surface defects of MgF_2 they would suffer a substantial deformation, such axially deformed tetrahedra giving an ESR signal similar to that observed as Mo(V) in $CdMoO_4$ (*14*). In the present work we did not observe such a complex in reduced samples of $MFMo_1$ and $MFMo_5$. Apparently there is little deformation of $[MoO_4]$ tetrahedra on the surface of MgF_2. In the reduced MoO_3–MgF_2 samples we observed octahedrally coordinated Mo(V), which formed a complex of square pyramidal symmetry with oxygen ligands. Such a complex is produced as the result of removal of oxygen from MoO_3 clusters formed at the surface of MgF_2. Molybdenum trioxide has a crystal structure in which the Mo ion is surrounded by six oxygen ions in strongly deformed octahedral surroundings with Mo–O bond lengths in the range 1.67–2.33 Å (*15*). The deformation of the octahedra results from the structure of molybdenum *d* orbitals and their redox potential relative to the anion valence band edge (*16*). In the octahedral coordination of oxide ions, in which d^2sp^3 hybridized orbitals are used by the metal to form σ bonds, the remaining d_{xy}, d_{yz}, and d_{xz} orbitals extend far enough to considerably overlap the πp orbitals of oxygen. As a result, π bonds with oxygen atoms are formed and the cation becomes displaced from the center of the octahedron toward terminal oxygen atoms. A modification of the electronic charge on oxygen ions takes place. The oxide ion toward which the cation is displaced becomes less basic, whereas all other oxide ions become more basic, the most basic being the oxide ion in the *trans* position.

The conclusion may thus be drawn that the surface of MgF_2 is partially covered with isolated tetrahedral species [MoO_4] and partially bears a layer of MoO_3 structure. A comparison of ionic radii and charges in MgF_2 (*4*), MoO_3 (*12, 14, 15*), and tetrahedral [MoO_4] (*9, 14*) leads to the conclusion that Mo incorporation into the octahedral site of Mg in the MgF_2 crystal lattice is very unlikely. Indeed, although the ionic radii of Mg and Mo differ considerably, X-ray diffraction patterns did not indicate any differences in lattice parameters of magnesium fluoride after impregnation with molybdate. Therefore, it can be concluded that Mo was not incorporated into the MgF_2 lattice, and remained located only at the surface of the fluoride.

Magnesium fluoride crystallizes in the rutile-type structure in which each Mg^{2+} ion is surrounded by six F^- ions and each F^- ion by three Mg^{2+} ions. The surroundings of a cation have the shape of a distorted octahedron; two fluoride ions are located at a slightly longer distance than the four remaining ones:

4(Mg–F) 1.94 Å
2(Mg–F) 1.99 Å

One can assume that the most frequently appearing lattice planes in MgF_2 are the close-packed planes occupied by both Mg^{2+} and F^- ions, namely the (001) plane (Fig. 3A) and the (110) plane (Fig. 3B). The remaining low-index planes are filled only with Mg^{2+} ions. In the coordination shell of each Mg^{2+} ion located in the (110) plane, one or two fluorine atoms are missing [Mg^{2+} ions with coordination number (C.N.) 5 or 4, respectively], whereas in the (001) plane besides coordinatively unsaturated ions Mg_{cus} (with coordination numbers as above), coordinatively saturated ions are also present. Electrical charges of Mg_{cus} ions are not balanced by the surrounding negative ions and amount to $+\frac{2}{3}$ for Mg^{2+} ions with C.N.-4 and to $+\frac{1}{3}$ for magnesium

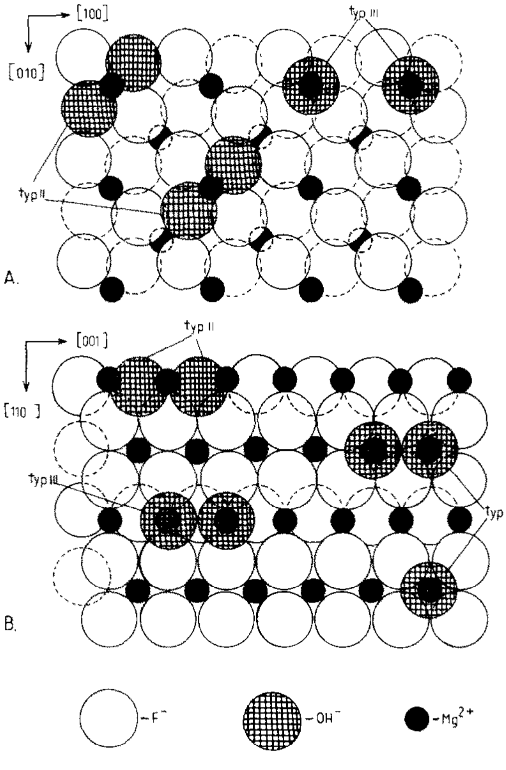

FIG. 3. The arrangement of OH groups on the surface of magnesium fluoride. (A) the (001) crystal face. (B) (110) crystal face.

ions with C.N. = 5. During the preparation of magnesium fluoride, or when it is contacted with water vapor, water dipoles interact with Mg_{cus} ions and fill their coordination sphere. This leads to the formation of surface hydroxyl groups. Three types of OH groups may be distinguished at the surface of MgF_2:

(1) Type I represents an OH group situated directly over an Mg^{2+} ion with C.N. = 5. The Mg–OH bond is perpendicular to the lattice plane.

(2) Type II corresponds to an OH group located between two Mg^{2+} ion, with two fluoride ions missing in the cation coordination sphere (C.N. of magnesium ion = 4). The Mg–OH bond forms an angle with the lattice plane.

(3) Type III is an OH group situated over a magnesium ion with C.N. = 4. The Mg–OH bond is perpendicular to the lattice plane.

The three types of hydroxyl group differ in electrical charge as well as in geometrical configuration. The charges of OH groups, as calculated from a simple ionic model, are $-\frac{2}{3}$ for type I, $-\frac{1}{5}$ for type II, and $-\frac{3}{5}$ for type III. As a result, the groups differ also in their properties. The Brønsted acidity of the OH groups diminishes and their basicity increases when their electrical charges become more negative (*17*). All three types of OH groups are basic. At the (001) surface plane of MgF_2, type II and III OH groups occur (Fig. 3A), while at the (110) plane, type I, II, and III OH groups are formed (Fig. 3B).

The presence of the there types of OH groups at the surface of magnesium fluoride is confirmed by the IR results in the OH stretching region (spectrum 1, Fig. 6). As can be clearly seen in the spectra of MgF_2 in this region three bands are present at 3770, 3620, and 3400 cm^{-1}, which may be assigned to OH groups of types II, I, and III, respectively (*4*).

The possible structures of surface species formed on impregnation of these two crystal planes of MgF_2 with molybdate ions may now be analyzed. Comparison of the ionic radii of Mg^{2+} (0.65 Å) and F^- (1.36 Å) in the magnesium fluoride lattice (*4*) with the size of Mo–O octahedral (*13, 14*) and tetrahedral groups (*13*) suggests the structure shown in Fig. 4 for the MoO_3–MgF_2 system. Figure 4A shows how separated $[MoO_4]$ tetrahedra may be located at the (001) lattice plane of MgF_2, and Fig. 4B represents the situation at the (110) plane. The tetrahedron marked "a" is coordinated to the surface through its apex oxygen ion, replacing the type III OH group linked to an Mg_{cus} ion. The edge of the tetrahedron marked "b" in Fig. 4B is located on two Mg_{cus} ions formed after removal of the OH group of type III, whereas the tetrahedron marked "c" (Fig. 4A) may be formed at the (001) plane as a result of its coordination with two Mg_{cus} ions with hydroxyls of type II removed. Figure 4C illustrates the arrangement of $[MoO_4]$ tetrahedra situated at the (001) plane of MgF_2 viewed from the $(\bar{1}10)$ direction. Moreover, the arrangement of Mg_{cus} ions in the (001) lattice plane in MgF_2 is also favorable for the formation of $[MoO_6]$ octahedral clusters. Conversely, such clusters cannot be formed at the (110) plane because distances between Mg_{cus} ions situated in this plane are too small. Figure 5 shows the way clusters of $[MoO_6]$ octahedra may be located at the (001) plane in MgF_2. They are formed by polymerization of $[MoO_4]$ tetrahedra, coordinated through their apex oxygen atoms to Mg_{cus} ions, as a result of the replacement of type III OH groups. The double-bonded oxygen ion is located in one of the apices of the octahedron parallel to the (001) plane. The axes of octahedra coordinated in this way are parallel to the (001) plane in MgF_2 and edge-linked MoO_6 octahedra in this plane form a laminar structure (Fig. 5). It may be estimated that the coverage of the MgF_2 surface with the layer of $[MoO_6]$ octahedra would be equivalent to 17% of a monolayer for $MFMo_1$ and 74% for $MFMo_5$, whereas in the case of $MFMo_{10}$ a multilayer must be

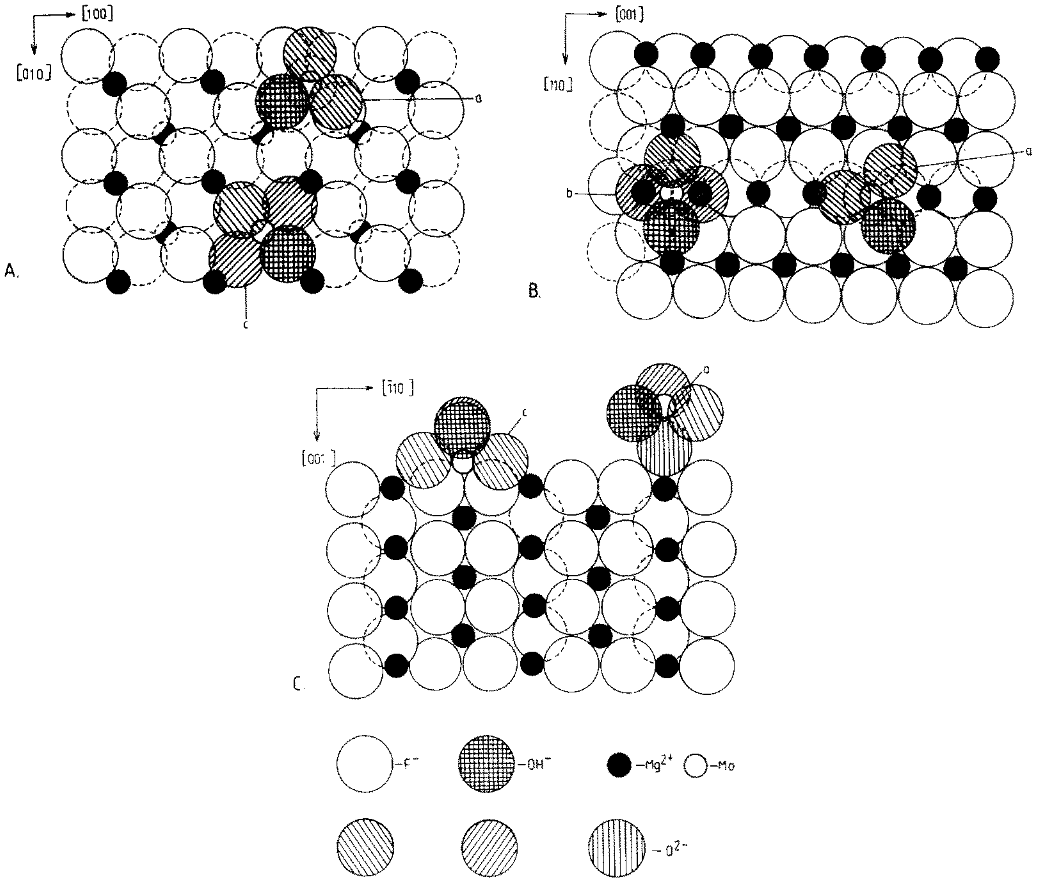

FIG. 4. [MoO_4] Tetrahedra located on MgF_2 surface; (A) (001) crystal face; (B) (110) crystal face; (C) tetrahedra on the (110) plane viewed along [001] and [$\bar{1}$10].

formed (132%). Consequently, the surface of the first two preparations may be covered partially with clusters of [MoO_6] octahedra and partially with isolated tetrahedra [MoO_4]. In reduced MoO_3–MgF_2 preparations Mo(V) was observed in the form of a complex characterized by a square pyramidal symmetry of oxygen ligands. Keeping in mind the MoO_3 lattice structure (*12*), one can expect that the only oxygen ion that can be removed is the surface oxygen bridging two adjacent octahedra. This is pictured in Fig. 5 in which the oxygen vacancy is shown as a small square. Removal of the oxygen ion leaves a reduced cation in square pyramidal coordination with double-bonded oxygen in the opposite apex as detected by ESR. Formation of such an oxygen vacancy suggests that the structure of the layer present on the surface of MgF_2 is identical to that of MoO_3.

Formation of isolated tetrahedral [MoO_4] groups and clusters of octahedra of the MoO_3 structure at the surface of the fluoride must cause some changes in the structure of surface hydroxyl groups in MgF_2 itself. As has already been shown, three types of OH group exist on the MgF_2 surface which differ in their electrical net charges and geometrical configuration.

Introduction of ammonium molybdate to a freshly precipitated magnesium fluoride to form $MFMo_2$ involves a considerable broadening of the 3620 cm^{-1} band and appearance of new bands with maxima at 3665, 3760, 3830, and 3900 cm^{-1} (spectrum

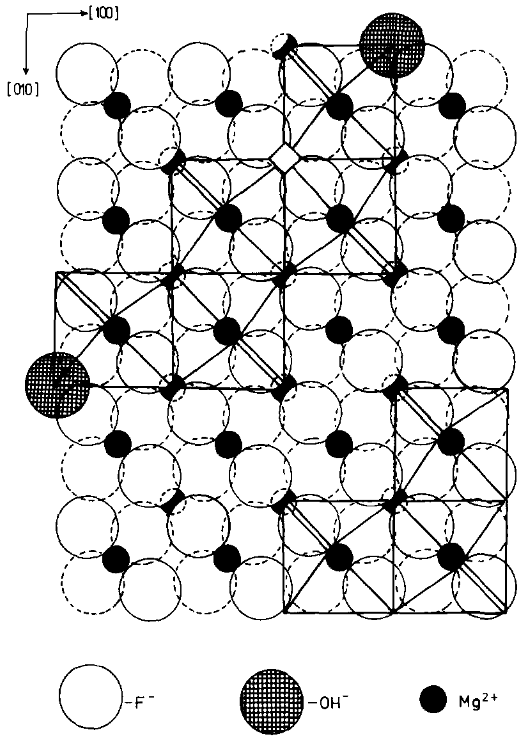

FIG. 5. Clusters of [MoO_6] octahedra on MgF_2 surface located in the (001) crystal face.

2, Fig. 6). The 3760 cm^{-1} band seems to be identical to that at 3770 cm^{-1} in pure MgF_2 (spectrum 1, Fig. 6). Enhancement of its intensity relative to the amount of Mo added results from the increase in the surface area of the MoO_3–MgF_2 preparations as new amounts of Mo are added. The 3900 and 3830 cm^{-1} bands may be assigned to isolated OH groups. The newly generated OH groups probably interact with OH groups of MgF_2 surface causing the broadening of the 3620 cm^{-1} band. More pronounced are the changes in the layer of surface OH groups for $MFMo_5$ (spectrum 3, Fig. 6). In the range of OH stretching vibrations the same bands recorded for $MFMo_1$ appeared, namely 3900, 3830, 3760, 3620, and 3400 cm^{-1}, whereas the 3665 cm^{-1} band split into bands at 3700 and 3640 cm^{-1}. The intensity of these bands increased in comparison with that of the bands for $MFMo_1$, which can be explained by the higher content of Mo. The sharpness of the lines at 3900 and 3830 cm^{-1} is evidence that no interaction takes place between the OH groups, which in turn indicates that they remain isolated. In contrast, bands of the other OH groups undergo broadening, which proves the interaction of these groups through hydrogen bonding. OH groups corresponding to 3760, 3620, and 3400 cm^{-1} bands were detected on the surface of the pure MgF_2; thus it may be assumed that they are linked with the surface Mg ions. The appearance of new bands at 3900, 3830, 3700, and 3640 cm^{-1} must be related to the Mo ions introduced onto the surface. For other preparations, i.e., $MFMo_{10}$, $MFMo_{18}$, and $MFMo_{25}$, the bands of OH groups are not as well resolved as for $MFMo_5$ since they contained

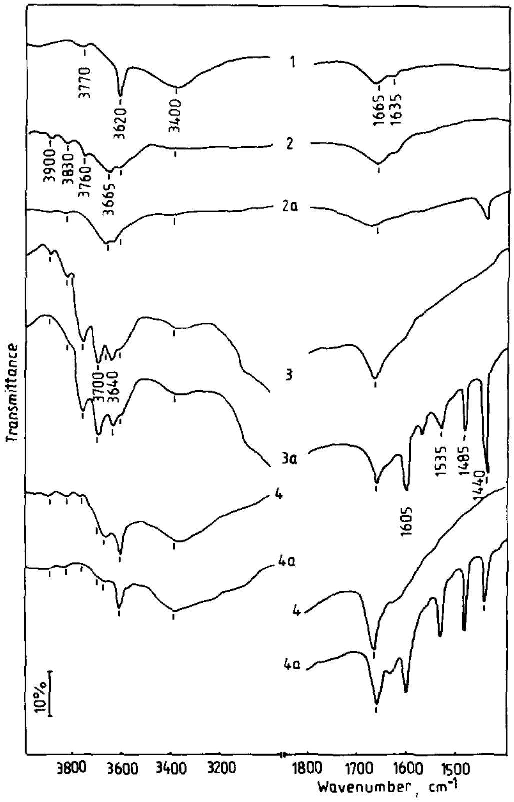

FIG. 6. IR spectra of MoO_3–MgF_2 samples before pyridine adsorption: (1) MgF_2, (2) $MFMo_1$, (3) $MFMo_5$, (4) $MFMo_{10}$. After pyridine adsorption: (2a) $MFMO_1$, (3a) $MFMo_5$, (4a) $MFMo_{10}$.

more MoO_3 and thus were characterized by smaller transmittance.

Besides the bands originating from OH groups, some other bands attributed to adsorbed water molecules have been detected. Thus, in the region of the deformation vibrations of adsorbed molecular water in the case of MgF_2, a band appeared at 1665 cm^{-1} and was assigned to hydrogen-bonded water molecules; moreover, a much less intense band at 1635 cm^{-1} belongs to water molecules not linked by hydrogen bonds but interacting with magnesium ions on the MgF_2 itself. After ammonium molybdate was introduced these bands grew in intensity because of the considerable increase in surface area.

The IR spectra obtained after exposing the samples to pyridine vapor (Py) revealed the acidic properties of these samples (spectra 2a, 3a, and 4a, Fig. 6). A clear indication of Lewis acidity was the band at 1440 cm^{-1}, whereas the presence of Brønsted acidity was indicated by the characteristic band at 1535 cm^{-1}. After Py admission in the case of the $MFMo_1$ sample, only the 1440 cm^{-1} band appeared, which suggested the presence of centers coordinatively binding pyridine. The band characteristic of pyridinium ion was not recorded. In the case of all other samples, intensive bands originating from Lewis sites as well as an intense band due to pyridinium ion were recorded. The behavior of different OH groups can most easily be studied by analyzing the bands of Py adsorbed on $MFMo_5$ (spectrum 3a, Fig. 6). The admission of Py brought about the disappearance of the 3900 and 3830 cm^{-1} bands. Hence, hydroxyls corresponding to these bands interact with Py, yielding pyridinium ion. Since these OH groups were not detected at the surface of MgF_2, they must be generated by the introduction of Mo–O polyhedra on the MgF_2 surface. None of the remaining OH groups present on $MFMo_5$, i.e., 3760, 3700, 3640, and 3620 cm^{-1}, changed their intensity after Py admission, which might indicate that these OH groups are weakly acidic or even nonacidic.

The most acidic properties should be related to OH groups bonded with tetrahedral Mo of the "c" type (Fig. 4A), because of their having the highest positive charge. The oxygen ions of a $[MoO_4]$ tetrahedron of this type are coordinated by two Mg_{cus} ions with unsaturated electrical charges amounting to $\frac{2}{3}$ unit for each Mg ion (after removal of two OH groups with charges amounting to $-\frac{1}{5}$ unit). As a result the electron cloud is shifted toward the oxygen ions bonded to Mg_{cus} ions, enhancing the acidic properties of the proton which neutralizes the $[MoO_4]$ tetrahedron. The OH group bonded with tetrahedral Mo, marked "b" in Fig. 4B, should exhibit a lower positive charge, which can result from solvation of the $[MoO_4]$ tetrahedron. This tetrahedron is coordinatively bonded with two Mg_{cus} ions after replacing the hydroxyl groups of type III, which have a charge of $-\frac{3}{5}$. It may be assumed that these two types of positively charged OH group give rise to the IR bands at 3830 and 3900 cm^{-1}, which were found to interact with pyridine, yielding pyridinium ions.

The negative charge of hydroxyl groups bonded with tetrahedral Mo in species marked "a" in Figs. 4A and B suggests their basic nature. The apex oxygen ion of this tetrahedron is located on an Mg_{cus} ion of electrical charge equal to $+\frac{2}{3}$. The band at 3700 cm^{-1} could be attributed to these OH groups.

The OH groups can also be coordinated with octahedral Mo, their properties being similar to those of weakly acidic hydroxyl groups present on molybdenum oxide (*8*). The 3640 cm^{-1} band may be assigned to these groups. An example of such hydroxyls bonded with octahedral Mo is the OH groups located in the outermost apices of the clusters of the monolayer of $[MoO_6]$ octahedra of MoO_3 structure (cf. Fig. 5).

Some additional information comes from IR spectra of adsorbed acetic acid. Acetic acid has been used as a reagent for the determination of the basicity of Al_2O_3 (*18*), MgF_2 (*4*), and zeolites (*19*). A spectrum of acetic acid adsorbed at 150°C on MgF_2 (spectrum 2, Fig. 7) points to merely insignificant changes in the intensities of the bands occurring in the region of the stretching vibrations of hydroxyl groups. On the other hand, when acetic acid was adsorbed at 250°C (spectrum 3, Fig. 7), the band at 3400 cm^{-1} disappeared and bands of OH groups in the range 3500–3800 cm^{-1} overlapped, forming one broad intense band. Simultaneously, at both temperatures strong bands originating from acetate ion (1610 and 1485 cm^{-1}) were observed. This would suggest that the OH groups are too weakly basic to interact with the acid at 150°C. The presence of acetate ions at this temperature indicates the existence of basic centers which could be the oxide and/or fluoride anions forming surface defects. They are stronger basic centers than the basic OH groups (3400 cm^{-1} band) which chemisorb acetic acid at higher temperature, namely at 250°C. A broadening and an increase in intensity of the band with a maximum at 3670 cm^{-1} result from the appearance of new OH groups on the surface, which in turn were formed as the result of the interaction of acidic protons with surface oxide ions. Thus, contrary to MgF_2, where the OH groups do not contribute significantly to surface basicity (*4*), hydroxyl groups on magnesium fluoride modified with ammonium molybdate, or at least some of them, can react as basic sites when contacted with acetic acid.

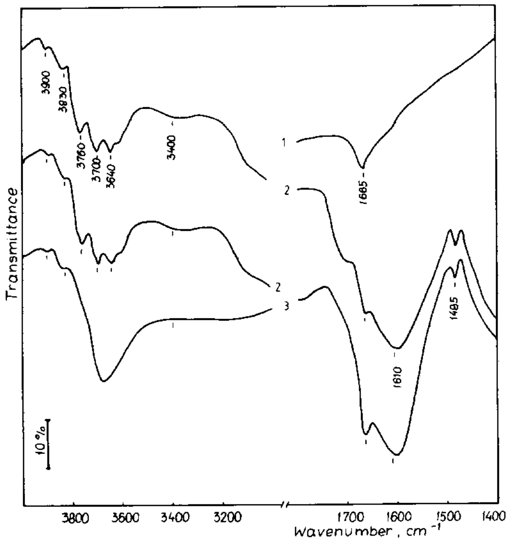

FIG. 7. IR spectra of $MFMo_5$ sample, before (1) and after acetic acid adsorption (2) at 150°C at 250°C.

It can therefore be concluded that a considerable change in MgF_2 surface properties took place after the molybdate ions were introduced. Strong Lewis acidity and strong Brønsted acidity appeared in the MoO_3–MgF_2 preparations. The contribution of proton acidity to the total acidity was significant; for example, for $MFMo_{10}$ and $MFMo_{18}$, proton acidity was 42 and 47% of the total acidity, respectively. Brønsted acidity in MgF_2 samples modified with Mo–O polyhedra comes from OH groups which are primarily hydroxyls bonded to Mo ions in tetrahedral coordination. Moreover, as they react with pyridine to form pyridinium ions, they are stronger Brønsted acids than the OH groups existing on the pure MgF_2 surface. As to Lewis acidity, on the other hand, this may result from the presence of coordinatively unsaturated Mo and/or Mg ions which form as a result of the dehydroxylation of the surface. Coordinatively unsaturated ions, in particular those of molybdenum, act as acceptor sites. A modification of the Lewis acid sites present on the pure MgF_2 surface may also contribute to the Lewis acidity of the MoO_3–MgF_2 system. The acidic strength of these centers may be enhanced as the result of a shift in electron density toward Mo; i.e., an increase in the acidic strength of Mg_{cus} ions due to interaction with Mo may be brought about. Two adjacent coordinatively unsaturated ions constitute a stronger acid center than a single coordinatively unsaturated ion.

The above-mentioned structural changes have a profound influence on the catalytic properties. All the samples with proton centers were active in cumene cracking (curve 2, Fig. 8). $MFMo_{18}$ proved to be the most active, and also had the highest ratio of protonic to aprotonic acidity per square meter at 350°C. Thus, introduction of ammonium molybdate to MgF_2 generated strong proton centers, in agreement with the previous results obtained for the MoO_3–Al_2O_3 system (*20*), where the introduction of MoO_3 also brought about an enhancement in proton acidity.

All the samples under study, even $MFMo_1$ with the lowest MoO_3 content, proved to be active for cyclohexene isomerization (curve 1, Fig. 8). For the most active ($MFMo_5$), the activity reached 3.7×10^{-7} mol/m² s·atm and was high in comparison with the activity of MgF_2 modified with H_3PO_4 and H_3BO_3 (*2, 3*). $MFMo_5$ had a low cumene cracking activity and small number of proton centers. Apparently in the case of this catalyst, the Lewis acidic centers are responsible for the catalytic activity. They must be strong enough to catalyze the cyclohexene skeletal isomerization which requires strong acidic centers. Catalysts with Mo/Mg > 0.05 were less active in this reaction, their activity diminishing with increasing amount of Mo, although they still remained more active than any of MgF_2 samples impregnated with acids (*2, 3*). The activity of MoO_3–MgF_2 for cyclohexene isomerization should be linked to the presence of Lewis-type acid sites. As mentioned above, the Lewis acidity of the samples originates from coordinatively unsaturated molybdenum ions or from magnesium ions. The pairs Mg_{cus}–Mo_{cus} ion pairs in particular may act as strong Lewis centers responsible for the activity of MoO_3–MgF_2 in this reaction. Their surface concentration attains a maximum for samples with atomic ratio Mo/Mg ~ 0.05, because at higher loadings the surface becomes covered with clusters of MoO_3.

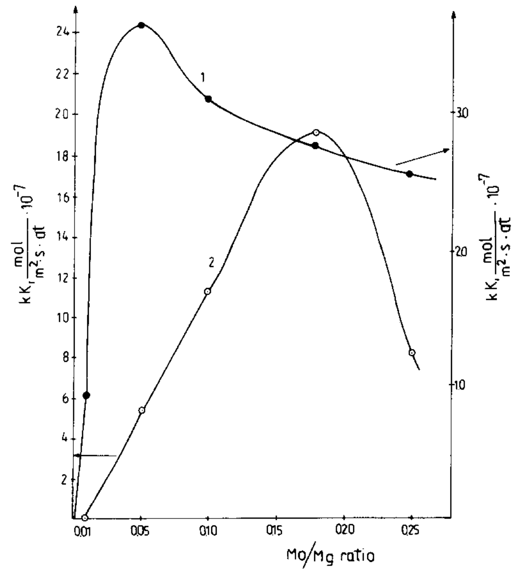

FIG. 8. Dependence of the activity for cyclohexene skeletal isomerization (curve 1) and the activity for cumene cracking (curve 2) on Mo/Mg atomic ratio.

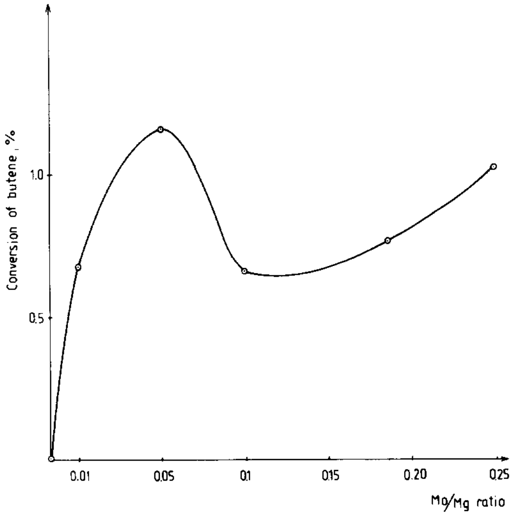

FIG. 9. Catalytic activity for 1-butene isomerization as a function of Mo/Mg atomic ratio.

MoO_3–MgF_2 also proved very active in the reaction of butene double-bond isomerization (Fig. 9). This reaction may proceed both on acid sites (of moderate strength) and on basic sites. Introduction of molybdate species to MgF_2 caused the appearance of catalytic activity for this reaction for all the samples. The activity of $MFMo_5$ was very similar to that of MFS_{18} described elsewhere (*1*), which was prepared by impregnation of MgF_2 with H_2SO_4 and was the most active among the MgF_2 catalysts promoted with acids. The highest conversion for this reaction was shown by $MFMo_5$ and $MFMo_{25}$. The reaction is assumed to proceed on acid centers of MoO_3–MgF_2 via butyl carbonium ion as intermediate, since in our experiments the *cis*-2-butene/*trans*-2-butene ratio was close to unit (0.7 to 1.2). If reaction occurred on basic centers via the π-allyl carbonium anion as intermediate, the ratio would have been higher (*21*). Apparently, the surface concentration of weak acid centers responsible for this reaction does not depend on the loading with molybdate ions. It should be stressed that the activities of all the samples under study for the reactions discussed are first-pulse activities.

Results of the investigation of oxidative ammonolysis of toluene are presented in Fig. 10 and Table 2. $MFMo_1$ already showed considerable conversion (25.3% benzonitrile). For all the other samples the initial conversion was very high and ranged from 58.1% for $MFMo_{25}$ to 68.6% for $MFMo_{10}$.

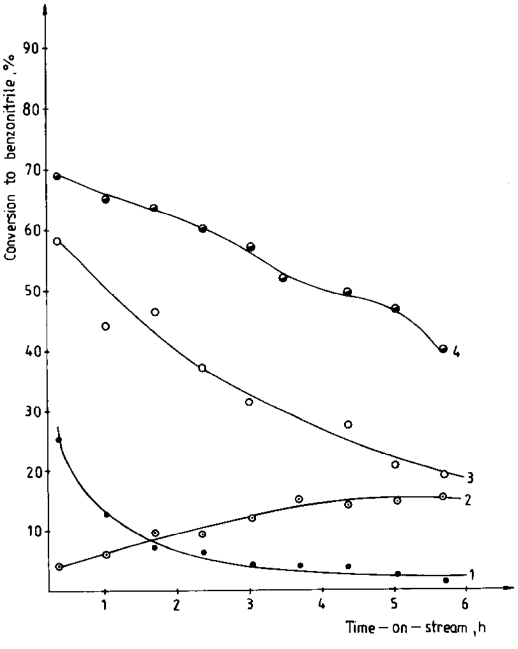

FIG. 10. Activity for toluene ammoxidation: (1) $MFMo_1$, (2) MoO_3, (3) $MFMo_{25}$, (4) $MFMo_{18}$.

TABLE 2

Catalytic Activity for Toluene Ammoxidation

Catalyst	Conversion to benzonitrile (%)		Coke deposit (wt%)
	Initial	Final	
MF	0.0	0.0	0.0
$MFMo_1$	25.3	1.3	5.3
$MFMo_5$	63.6	41.6	4.0
$MFMo_{10}$	68.6	40.1	5.3
$MFMo_{18}$	67.0	35.1	6.2
$MFMo_{25}$	58.1	19.2	8.3
MoO_3	4.1	15.2	—[a]

[a] Not determined

During the 6-h process a gradual decrease in conversion could be observed. The decrease is linked to the deposition of coke blocking active centers. The relationship between coke content (wt%) and decrease in activity after 6-h time-on-stream is nearly linear.

Pure MgF_2 proved to be completely inactive in ammoxidation, whereas the activity of MoO_3 gradually rose to attain after 4 h a stable level of ca. 15% conversion to benzonitrile. Thus, the activity of the MoO_3–MgF_2 samples is linked to the presence of MoO_3 in catalysts.

Ammoxidation processes have been studied by many researchers (*16, 22–27*). In examining the oxidation processes on V_2O_5/Al_2O_3, some authors (*23–25*) assumed a bifunctional behavior of the catalyst, ascribing its oxidizing properties to V_2O_5 and dehydration to Al_2O_3. A similar mechanism could be assumed for MoO_3–MgF_2. In this mechanism toluene would be oxidized on MoO_3 to the $PhCOO^-$ ion, which migrates to the MgF_2 surface to be stabilized there as the benzoate ion (Ph-COOMg). On interaction with MgF_2, ammonia gives $MgO^-NH_4^+$ which subsequently reacts with the benzoate ion to give benzonitrile. The reduced centers present on MoO_3 would easily be reoxidized with molecular oxygen.

In view of the recent progress made in understanding the mechanism of ammoxidation of propylene (*16, 22*), the analogy between the behaviors of propylene and toluene can be exploited to propose a mechanism of ammoxidation of toluene on MoO_3–MgF_2. Thus, one may propose the following:

(i) A toluene molecule in the first step undergoes dissociative chemisorption. Such chemisorption requires the participation of two centers: one, an oxygen ion of the catalyst surface, adsorbs the hydrogen atom; the other centre, e.g., an Mo ion, forms a bond with the benzyl radical. As a result, a surface complex of type I is formed:

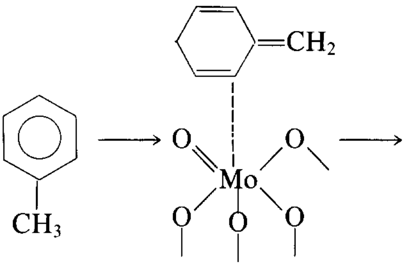

(I)

(ii) In the presence of ammonia, a nucleophilic attack of the NH^{2-} group, replacing O^{2-} ion in the MoO_3 lattice, takes place:

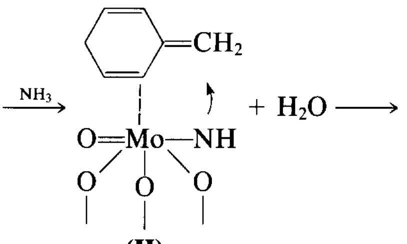

(II)

(iii) The resulting surface complex (II) undergoes rearrangement into **III**:

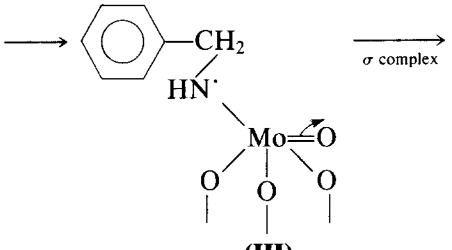

(III)

(iv) subsequent abstraction of two hydrogen atoms leads to formation of adsorbed benzonitrile **(IV)**:

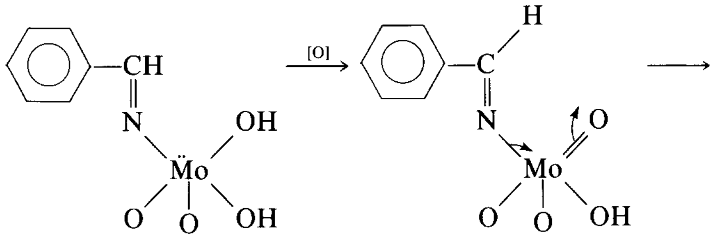

(IV)

(v) In the next stage decomposition of the complex thus formed takes place, together with desorption of the benzonitrile molecule.

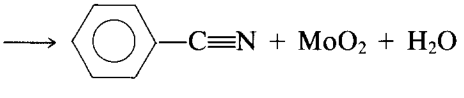

(vi) Oxygen taken from the catalyst surface in the ammoxidation process is then replaced with molecular oxygen, which reactivates the active centers. In this way the redox cycle is completed.

Summing up the results of this study, we can say that introduction of molybdate species to magnesium fluoride brings about changes in the MgF_2 surface composition. Isolated tetrahedra $[MoO_4]$ and clusters of $[MoO_6]$ octahedra of MoO_3 structure formed on the fluoride surface modify the acid-base as well as redox properties of MgF_2. On MoO_3–MgF_2 samples, considerable enhancement of both Lewis and Brønsted acidity takes place, which results in the appearance of catalytic activity in such reactions as cumene cracking, skeletal cyclohexene isomerization, and butene double-bond isomerization. Contrary to the effect of acids on MgF_2 surface (where Lewis acidity appears nearly exclusively), the acidity that forms in this case is of both Lewis and Brønsted type. Introduction of Mo–O polyhedra to the MgF_2 surface also generates strong oxidizing properties. This is manifested by high activity of MoO_3–MgF_2 samples in the toluene ammoxidation process.

REFERENCES

1. Wojciechowska, M., *Pol. J. Chem.* **53,** 1829 (1979).
2. Wojciechowska, M., *Bull. Acad. Pol. Chim.* **28,** 237 (1980).
3. Wojciechowska, M., *Bull. Acad. Pol. Chim.* **29,** 549 (1981).
4. Wojciechowska, M., *Bull. Acad. Pol. Chim.* **29,** 533 (1981).
5. Przystajko, W., Fiedorow, R., and Dalla Lana, I. G., *Appl. Catal.* **15,** 265 (1985).
6. Fiedorow, R., Kania, W., Kuczyński, W., and Więkowski, A., *in* "Proceedings, Fifth International Congress on Catalysis, 5th (Florida 1972)," p. 1455. North-Holland, Amsterdam, 1973.
7. Bassett, D. W., and Habgood, H. W., *J. Phys. Chem.* **64,** 769 (1960).
8. Oganowski, W., Hanuza, J., Jeżowska-Trzebiatowska, B., and Wrzyszcz, J., *J. Catal.* **39,** 161 (1975).
9. Clark, G. M., and Doyle, W. P., *Spectrochim. Acta* **22,** 1441 (1966).
10. Mitchell, P. C. H., and Trifirò, F., *J. Chem. Soc. A*, 3183 (1970).
11. Che, M., *J. Chem. Phys.* **71,** 1954 (1979).
12. Haber, J., *in* "The Role of Solid State Chemistry in Catalysis" (R. K. Grasselli, and J. F. Brazdil, Eds.), p. 3. Society Symposium Series. Amer. Chem. Soc., Washington, DC, 1985.
13. Zhan, R. Y., Narayana, M., and Kevan, L., *J. Chem. Soc. Faraday Trans. 1* **81,** 2083 (1985).
14. Martini, G., *J. Magn. Reson.* **15,** 262 (1974).
15. Burlamacchi, L., Martini, G., and Ferroni, E., *Chem. Phys. Lett.* **9,** 420 (1971).
16. Haber, J., *in* "Proceedings, International Congress on Catalysis, 8th (Berlin, 1984)," Vol. I, p. 85. Verlag Chemie, Weinheim, 1984.
17. Knözinger, H., and Ratnasamy, P., *Catal. Rev. Sci. Eng.* **17,** 31 (1978).
18. Szabo, Z. G., and Jover, B., *in* "Proceedings, International Congress on Catalysis, 5th (Florida 1972)," p. 833. North Holland, Amsterdam, 1973.
19. Bielański, A., and Datka, J., *J. Catal.* **32,** 183 (1974).
20. Laine, J., Brito, J., and Yunes, S., "Third Climax International Conference on Chemistry and Uses of Molybdenum" (H. F. Barry and P. C. H. Mitchell, Eds.), p. 111. Climax Molybdenum Company, Ann Arbor, MI, 1979.
21. Hattori, H., Ytoh, M., and Tanabe, K., *J. Catal.* **38,** 172 (1975).
22. Grasselli, R. K., and Burrington, J. D., *Adv. Catal.* **30,** 133 (1981).
23. Niwa, M., Ando, H., and Murakami, Y., *J. Catal.* **49,** 92 (1977).
24. Murakami, Y., Ando, H., and Niwa, M., *J. Catal.* **67,** 472 (1981).
25. Niwa, M., Ando, H., and Murakami, Y., *J. Catal.* **70,** 1 (1981).
26. Grzybowska, B., Haber, J., and Janas, J., *J. Catal.* **49,** 150 (1977).
27. Haber, J., and Grzybowska, B., *J. Catal.* **28,** 489 (1973).